Multifractality, multifractal phase transitions, and symmetry-increasing bifurcations in ac-driven phase-slip centers

Rafael Rangel and Luis E. Guerrero
Departamento de Física, Facultad de Ciencias, Universidad Central de Venezuela, Apartado 47588, Caracas 1041A, Venezuela and Centro de Física, Instituto Venezolano de Investigaciones Científicas, Apartado 21827, Caracas 1020A, Venezuela
(Received 3 May 1990)

Chaos at and beyond onset is studied for nonequilibrium current-carrying dissipative states in quasi-one-dimensional dirty superconductors. For the case of ac-driving currents, phase-slip center solutions of the generalized time-dependent Ginzburg-Landau equations show a universal transition at the onset of chaos. For currents below the onset, the pervasive feature is the nonhyperbolicity: homoclinic tangency between stable and unstable manifolds of unstable periodic orbits. Pointwise dimensions $\alpha(x)$ evaluated on the attractors show abnormally low values, indicating regions made of an overlapping of stable and unstable manifolds of saddle orbits. These regions cause a break of self-similarity and a phaselike transition in the multifractal probability measure of the attractor. Finally, one of these tangencies causes a symmetry-increasing bifurcation.

I. INTRODUCTION

The generalized time-dependent Ginzburg-Landau equations[1-4] (GTDGLE), which model dissipative states (nonequilibrium states in superconductivity), appear interesting in testing the universalities that exist at the borderline of chaos and for the study of chaotic phenomena beyond that. Until now most work, both experimental and numerical simulations, has concentrated on testing such universalities for the best known routes to chaos: the period-doubling and the quasiperiodic routes.[5-7] At the onset of chaos, dynamical systems exhibit qualitative and quantitative features that are universal.[8] Much less is known about generic behavior or any kind of supercritically universality, i.e., beyond onset. Recent theoretical work shows some universal features beyond onset, which has been confirmed experimentally for the quasiperiodic route.[9,10] However, rigorous theoretical work has only been possible recently for low-dimensional systems represented by discrete maps.

Much more difficult is the theoretical study of realistic models, which helps to explain experimental results.[3,4,11,12] In such cases a theory based on low-dimensional maps helps one to understand the results of numerical experiments of a complex system modeled by a nonlinear partial differential equation (NPDE). In a complex system of, in principle, infinite degrees of freedom, one can expect the gradual change from quasi-one-dimensional to higher-dimensional behavior or even a transition to some kind of turbulencelike state.[13]

In a previous work[14] (from now on referred to as I), the existence of ac-driven phase-slip centers (see below) was proved and some regions of the parameter space were explored. Furthermore, in that work the existence of period-doubling cascades of birfurcations to chaos was found, i.e., the transition to bounded and in general fractal objects with an attracting invariant set (strange attractors) and a fundamental neighborhood in an appropriate space of functions or phase space.

In this work we concentrate on the period-doubling scenario. We work on the last dissipative branch of the response diagram (Fig. 1). Our aim is to give a picture of dynamics as complete as possible at the onset of chaos and, most importantly, beyond onset. For that purpose we calculate the generalized dimensions D_q and the multifractal spectrum of scaling indexes $f(\alpha)$ at the transition to chaos on the low-current side of the response.

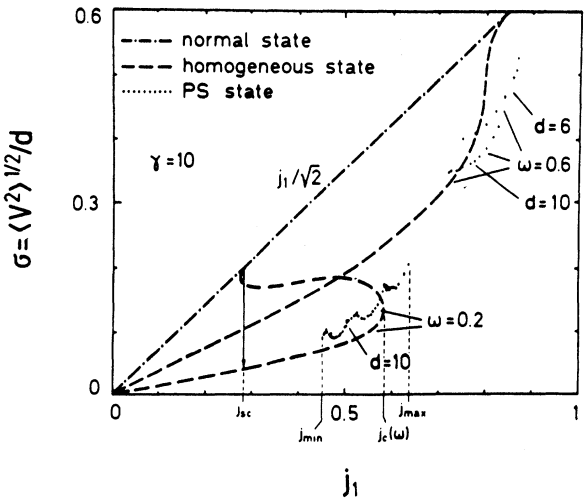

FIG. 1. The quantity σ (see Chap. V) is plotted as a function of j_1 for $\omega=0.6$ and 0.2, $\gamma=10$. The values for the homogeneous state are calculated numerically and analytically [Eqs. (9)–(11), paper I]. The arrow indicates the value of the current j_1 for $\omega=0.2$, where the normal state becomes linearly unstable. This was shown in I. We work on the low-current side for PS states which begin before the last symemtry-breaking bifurcation occurs, i.e., $j_1\approx 0.49$, and ends with $j_{\min}$ where the PS state becomes unstable.

Here the last symmetry-breaking bifurcation takes place. This bifurcation leads to a period-doubling cascade (see Figs. 5–7 in I) resulting in a strange attractor. We construct local Poincaré maps (LPM) using as variables the chemical potential μ (which gives the total voltage generated by the nonequilibrium state along the filament and the phase ϑ of the order parameter ψ at the place where it goes to zero [named a phase-slip center[1] (PSC)], i.e., we construct the two-dimensional map defined by $(\vartheta(x=0,\ t=nT_\omega),\ \mu(x=0,\ t=nT_\omega))$. Our results show that this transition to chaos is of the same kind as the one studied for the class of unimodal maps of the interval and therefore, in that sense, it is universal.[8] We also study the multifractality beyond onset. Many features of the behavior near and beyond the onset can be explained by using the logistic map because the regime is strongly dissipative. However, the facts that locally (at $x=0$) the degrees of freedom are 3, $|\psi(0,t)|$, $\mu(0,t)$ and $\vartheta(0,t)$, and that there is a local symmetry (see below), lead us to consider a two-dimensional Hénon-like model with the same local symmetry. Some aspects of this model have been studied by Yamaguchi and co-workers.[15] Many features of the scenario found beyond the onset of chaos can be explained qualitatively with that model. Especially important features are the gradual foliation (attractor widening) of the chaotic attractors defined through the LPM [Eq. (17)], as the control parameter [the amplitude of the ac-driving current j_1 in Eq. (3)] is lowered and the existence of a symmetry-increasing bifurcation (SIB). That remarkable phenomenon—the appearance of a chaotic attractor which has on average the full local symmetry, i.e., the natural measure has symmetries—has been pointed out by Chossat and Golubitsky.[16]

The most pervasive features of the scenario after onset are the homoclinic tangencies between the stable and unstable manifolds of saddle orbits. Analysis of the pointwise dimensions or microscopic information [Eq. (24)] on the chaotic attractors shows that there are such tangencies. Therefore, the Poincaré map behaves as a two-dimensional nonhyperbolic map for a range of currents. Intermittence is a feature that is always present near the bifurcating values of j_1 where a homoclinic tangency occurs. Especially, the intermittency at the SIB is rather robust. Such tangencies cause the breaking of the self-similarity[17,18] and a phaselike transition in the fractal measure as well as the gradual widening of the attractors (foliation). Finally, the LPM ceases to be two dimensional, and other degrees of freedom soften.

The scenarios we have found beyond the onset of chaos are, we believe, not special to the system we are studying but have *generic relevance* and could be found in other complex systems described by NPDE. There is evidence that this is the case for the system studied in Ref. 19.

The paper is organized as follows. In Sec. II we give the GTDGL equations, explain some facts concerning the symmetries, and define the LPM. In Sec. III some basic properties of the ac-driven phase-slip-center solutions are given. In Sec. IV we explain in some detail how we calculate the partition function [Eq. (19)], which we use to obtain the multifractal spectrum $f(\alpha)$. We also give the theoretical framework we use to analyze the results. In Sec. V we present the results at onset. Section VI is devoted to the phase transitions and the symmetry-increasing bifurcation. In Sec. VII we give a discussion of the results and make a connection to other work based on questions derived from this paper.

II. THE GENERALIZED TIME-DEPENDENT GINZBURG-LANDAU EQUATIONS

The application of nonequilibrium transport theory to dirty superconductors has been a successful enterprise.[4,12,20,21] Our theoretical objects are thin and long current-carrying filaments [with transverse dimensions that are small compared to the coherence length $\xi(T)$ and the penetration depth $\lambda(T)$] near T_c in a temperature range where the local-equilibrium approximation is valid for dirty superconductors. Then, the magnetic field of the current can be neglected. Our filaments are then described by the GTDGL equations (for a review see Ref. 3),

$$u(1+\gamma^2|\psi|^2)^{-1/2}(\partial_t+i\mu+\gamma^2\partial_t|\psi|^2)\psi = (\partial_x-iA)^2\psi+(1-|\psi|^2)\psi\ , \tag{1}$$

$$j=[\mathrm{Im}(\psi^*\partial_x\psi)-A|\psi|^2-\partial_x\mu-\partial_t A]\ , \tag{2}$$

$$j(t)=j_0+j_1\cos\omega t\ . \tag{3}$$

Here $\psi=\Delta/\Delta_0(T)$ is the complex order parameter, $j(t)$ the current density, μ the scalar potential, A the x component of the vector potential, and $u=\pi^4/14\xi(3)=5.79$. $\Delta_0(T)$ is the BCS order parameter,

$$\Delta_0(T)=\left[\frac{8\pi^2T_c^2}{7\xi(3)}\left[1-\frac{T}{T_c}\right]\right]^{1/2},$$
$$\xi(T)=\left[\frac{8T_c}{\pi D}\left[1-\frac{T}{T_c}\right]\right]^{-1/2}, \tag{4}$$
$$\gamma=\frac{2\tau_E\Delta_0(T)}{\hbar}=\gamma_0\left[1-\frac{T}{T_c}\right]^{1/2},$$

and

$$\gamma_0=\frac{8u^{1/2}}{\pi}\frac{k_BT_c\tau_E}{\hbar}$$

is inversely proportional to the pair breaking by inelastic scattering (τ_E is the inelastic collision time). Lengths are measured in units of $\xi(T)$, whereas time and current are measured in units,

$$t_0=\pi\hbar/[8k_B(T_c-T)u],\quad j_0=\sigma_0\hbar/[2et_0\xi(t)] \tag{5}$$

(σ_0 is the normal conductivity). The electric field

$$E=-(\partial_x\mu+\partial_t A) \tag{6}$$

is measured in units of $\hbar/2et_0\xi$. The validity of the local-equilibrium approximation requires

$$|1-T/T_c|\ll u^{1/2}\gamma_0^{-1},\quad \omega\tau_E\ll 1 \tag{7}$$

(ω is the frequency in physical units). We will be dealing with frequencies such that $\omega t_0=\omega\approx 1$. This is within the

range of validity when $t_0 \gg \tau_E$, which is essentially equivalent to the first equation in (7).

Since the equations are invariant under the gauge transformation

$$\psi \to \psi \exp[-i\chi(x,t)], \quad \mu \to \mu + \partial_t \chi , \quad A \to A - \partial_x \chi , \tag{8}$$

one can choose gauges where $A \equiv 0$ or where $\mu \equiv 0$. For the sake of completeness the vector-potential gauge, which can sometimes be preferable (I), is given. With

$$\psi = F \exp(i\theta), \quad \phi = \mu + \partial_t \theta, \quad Q = \partial_x \theta - A \tag{9}$$

($F > 0$), Eqs. (1) and (2) go over into

$$u(1+\gamma^2 F^2)^{1/2} \partial_t F = \partial_x^2 F + (1 - Q^2 - F^2)F , \tag{10}$$

$$\partial_t Q = -F^2 Q + \partial_x \phi + j(t) , \tag{11}$$

$$uF^2 \phi = (1+\gamma^2 F^2)^{1/2} \partial_x (F^2 Q) . \tag{12}$$

However, the gauge-invariant potentials (GIP), $\phi = \mu + \partial_t \theta$ and $Q = \partial_x \theta - A$, are well defined only when $F \neq 0$, and one has to be careful in using this formulation of the TDGL equations in the presence of phase slips. In fact, the generalized potentials diverge at the moment of the phase slips. From now on we will consider ac applied currents ($j_0 = 0$)

$$j(t) = j_1 \cos \omega t \tag{13}$$

and choose the gauge with $A \equiv 0$ and a gauge with $\mu = 0$ at $x = d/2$, where d is the length of the filament. The total voltage along the filament is $V = 2\mu(0)$. We use periodic boundary conditions.

In I we have discussed some general aspects of the behavior to be expected for pure ac-driving ($j_0 = 0$) with emphasis on the case $\gamma \gg 1$, which is the important range for ordinary low-temperature superconductors. Also, the general features of the bifurcation scenario in the response diagram, $\gamma = 10$ and $\omega = 0.2$ (Fig. 1) were studied. We work here in the low-current side, $j_1 < 0.4790$.

The existence of symmetries help us to classify the solutions. To do this it is important to note that the basic equations (1), (2), and (3) with $j_0 = 0$ (unbiased case) are invariant under the transformations

$$t \to t + nT_\omega, \quad \psi \to \psi, \quad \mu \to \mu, \quad n = \pm 1, \pm 2, \ldots \tag{14}$$

$$t \to t + T_\omega/2, \quad \psi \to \psi^*, \quad \mu \to -\mu , \tag{15}$$

where $T_\omega = 2\pi/\omega$ is the time period. Solutions which possess the symmetry (15) are called "symmetric," otherwise "nonsymmetric" (I). Symmetric solutions always appear to possess the full set of symmetries, i.e., (14) with all integers n, at least so long as the solutions are periodic (see below). However, there are bifurcations from chaotic attractors where the full symmetry (15) is restored, but only on the average [symmetry-increasing bifurcation). In that case only symmetry (15) is present.

Clearly for symmetric solutions the Fourier series of μ has contributions only for odd multiples of ω ($|\psi|$ only for even multiples). Transitions from higher to lower symmetry involve continuous bifurcations. Each broken symmetry gives rise to a multiplicity of solutions connected by the symmetry transformations. The attractors related through (15) are called conjugated attractors. Which attractor the system settles into depends on the initial conditions.

The symmetry transformation (15) is equivalent to the following transformation for the phase of the ψ at $x = 0$:

$$\begin{aligned} &\vartheta(x=0,t) \to -\vartheta(x=0, t+(2n+1)T_\omega/2) , \\ &\dot{\vartheta}(x=0,t) \to -\dot{\vartheta}(x=0, t+(2n+1)T_\omega/2) \\ &\qquad = -\mu(0, t+(2n+1)T_\omega/2) . \end{aligned} \tag{16}$$

An infinite-dimensional Poincaré map can be defined at $x = 0$; it is given by

$$\begin{pmatrix} \vartheta(x=0,(n+1)/T_\omega) \\ \dot{\vartheta}(x=0,(n+1)T_\omega) \\ \vdots \end{pmatrix} = P \begin{pmatrix} \vartheta(x=0,nT_\omega) \\ \dot{\vartheta}(x=0,nT_\omega) \\ \vdots \end{pmatrix} . \tag{17}$$

Despite the fact that P is defined locally, i.e., at $x = 0$, it serves to characterize the whole solution. From (16) and (17) one deduces that P restricted to the first two components can be obtained as the second iteration of a map P^*.[22] Symmetric solutions are fixed points of P^*. As a result, symmetric solutions have only odd multiples of ω in the fast-Fourier transform (FFT) of $\mu(0,t)$, and its time average is zero, which means that such solutions do not show an average voltage $\bar{V}$. We use (17) projected to the first two variables and consider the map induced locally in that way. As long as the dimension of the attractors remains locally below 2 this map is well defined.

III. BASIC PROPERTIES OF ac-DRIVEN PHASE-SLIP-STATE SOLUTIONS

The spatial structure of the ac-driven PSC is similar to the isolated dc PSC.[2,4,14] The order parameter $\psi(x)$ is vortexlike, executing oscillations that go through zero at $x = 0$ and in general in an aperiodic way, in contrast to the limit cycle dc PSC. For symmetric periodic solutions the number of phase slips is always an integer number every half of the period. For nonsymmetric solutions, phase slips are no longer equidistant in time, but they pair up. Although $\mu(t)$ does not have the symmetry (16), the mean voltage $\langle V \rangle = \langle \mu(d/2) - \mu(-d/2) \rangle$ is still zero. In order to have $\langle V \rangle \neq 0$ there would have to be more phase slips in one sense of the rotation of the phase than in the other. To see this we note that as a consequence of the periodic boundary conditions at $x = \pm d/2$ the gauge-invariant potential $\phi = \mu + \partial_t \theta$ is zero at $x = \pm d/2$ [see Eq. (12)]. Therefore we have the Josephson relation

$$\begin{aligned} \langle V \rangle &= \mu(d/2) - \mu(-d/2) \\ &= \langle \partial_t \theta(-d/2) - \partial_t \theta(d/2) \rangle . \end{aligned} \tag{18}$$

In a stationary situation (limit cycle) a net relative rotation of the phase inherent in Eq. (18) must be compensated by phase slips.

On the low-current side, where one has one phase slip

per half-cycle, the solutions are fairly simple. The symmetric solutions exist in the range $0.501\,55 < j_1 < 0.49$ (In Fig. 5 of I, $j_1 = 0.5015$). At slightly higher currents one has chaotic solutions and the transition occurs via intermittency. At $j_1 = 0.49$ a symmetry-breaking transition occurs followed by a cascade of period-doubling bifurcations ending at $j_1 \cong 0.474\,892$.

IV. MULTIFRACTAL FORMALISM AND THE UNIVERSAL TRANSITION AT THE ONSET OF CHAOS

In order to obtain the generalization dimensions D_q and the multifractal spectrum of scaling indexes $f(\alpha)$, one calculates the partition function on the attractor defined as[8]

$$\Gamma(q,\tau,\{S_i\},l)=\sum_{i=1}^{N} \not{\kappa}_i^q \ . \tag{19}$$

Γ is formally analogous to the partition function $Z(\beta)$ in the thermodynamics. Its singularities define phase transitions.[23] In (19) the probability $\not{\kappa}_i$ is given by the natural measure on the attractor. It is given in the thermodynamic limit by defining a grid which covers the attractor, each box on the grid is labeled by i (S_i denotes the boxes which are not empty), and letting the box size l_i go to zero and N go to infinity. One has

$$\not{\kappa}_i(l)=\lim_{N\to\infty} N_i/N, \tag{20}$$

$$D_q=\frac{1}{q-1}\lim_{l\to 0}\frac{\ln\sum_i \not{\kappa}_i^q}{\ln l} \ , \tag{21}$$

where N_i is the number of times the time series visits the box as the numerical simulation of the equations goes on, i.e., $\not{\kappa}_i(l)$ is the probability that the trajectory on the attractor $X_1,\ldots,X_N$ visits the box labeled by i. The values X_i are defined by the P. That physical measure[24] is based on the fact that the time evolution [Eqs. (1), (2), and (13)] produces well-defined voltage averages [see after Eq. (13)]. In fact, the quantity $\sigma=(\langle\mu^2(0,t)\rangle)^{1/2}/d$ [Eq. (26) in I], shown in Fig. 1, defines the time average of the square of the voltage along the filament. It does not depend on the initial conditions and converges rapidly to a number which soon stabilizes in the first digits. As the time evolution goes on, σ becomes more precisely defined. Therefore, there is an ergodic probability measure on the attractor.[25] However, clearly l_i and N will be always finite in our calculation so that the probability of the box s_i and the partition function are given by[26]

$$\not{\kappa}_i \approx \int_{i\text{th box}} d\nu(x) \ , \tag{22}$$

$$\Gamma(q,l)=\int d\nu(x)[\nu(B_l(x))]^{q-1} \ . \tag{23}$$

$B_l(x)$ denotes a ball of radius l around x. $\nu(x)$ denotes the invariant measure.[25] There is a relation between the crowding index α_i (Ref. 27) and the natural measure $\not{\kappa}_i$ which scales as

$$\not{\kappa}_i \approx l_i^{\alpha_i(l_i)} \ . \tag{24}$$

In the limit $l_i \to 0$ one obtains the pointwise dimension around the resulting point $\alpha(x)$ according to the partition on the grid which must contain a point of the attractor in that limit. The number of times or boxes $n(l)$ that the quantity [defined by (24)] in the limit $l_i \to 0$ appears scales also as a power of l (The grid size) as

$$n(l)\approx l^{-f(\alpha)} \ , \tag{25}$$

where the index α without the suffix i denotes the common value. This gives rise to the interpretation that these boxes cover a subset of the attractor of fractal dimension $f(\alpha)$.[28] Therefore, we assume that the attractors are the union of fractal sets. The procedure to calculate the $f(\alpha)$ versus α curve would be to make log-log plots as one uses different scales l according to Eqs. (24) and (25); however, this procedure requires too many points and as we are simulating a partial differential equation the computational time would be enormous. For this reason we use the fact that the measure is ergodic so that the recurrence time approximation and averaging over all points of the attractor can be carried out,[29] i.e., we count the number of steps m_i at the trajectory, starting from a point labeled i and returning to it within a radius l, and set this number m_i equal to the probability measure $\tilde{\not{\kappa}}_i$, which gives the probability of finding the trajectory within the ball of radius l around the point X_i of the attractor. One has $\alpha_i(x)=-\ln m_i/\ln l$. Finally, after averaging over all points of the attractor the partition function turns our to be given by

$$\Gamma(q,l)=\langle\tilde{\not{\kappa}}_i^{\,q-1}\rangle\approx l^{\tau(q)} \ . \tag{26}$$

The different exponent of (26) as compared to (19) is due to averaging. (The brackets denote averaging.) The quantity $\tau(q)=(q-1)D_q$ is the scaling exponent of the partition function, as can be expected on general grounds.[8] However, other types of singularities can also exist which can give rise to other types of dimensions.[30] A better variant of the same method uses the measure[31]

$$\tilde{\not{\kappa}}_i(l)=\frac{1}{N}\sum_{j=1}^{N}\Theta(l-|X_j-X_i|) \tag{27}$$

so that

$$\Gamma(q,l)=\frac{1}{N}\sum_{i=1}^{N}\tilde{\not{\kappa}}_i(l)^{q-1} \ . \tag{28}$$

In numerical calculations the two methods are, with small changes, the same. Conceptually the recurrence time approximation is an approximation to the measure defined by (27). Let us remark that there is the possibility of attractor sets which are locally the product of independent structures along directions in two-dimensional phase space.[27] This is important because for hyperbolic systems one of these directions is given by the unstable manifolds. The attractors impose a continuum structure with partial dimension one along the unstable direction. For nonhyperbolic systems, where both stable and unstable directions can locally mix through tangencies, there may be a Cantor structure along both stable and unstable directions.

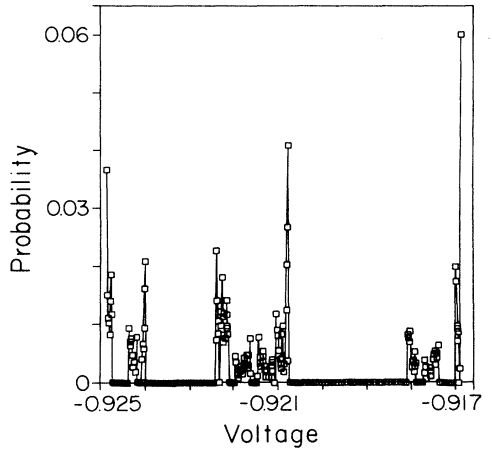

FIG. 2. The histogram showing the natural measure obtained from the values taken from the electric potential $\mu(0,nT_\omega)$. The measure resembles the measure of the Feigenbaum attractor.

V. RESULTS FOR J_1 AT ONSET AND SLIGHTLY BEYOND

We have found the value of the current at the onset of chaos by $j_1=j_{\rm ons}=0.474\,892$. We construct at that value a histogram and find a set which appears to be disconnected and remarkably resembles the Cantor set of the Feigenbaum attractor. The Poincaré map is one dimensional. At $j_1=0.474\,890$ islands have formed, as is shown in Fig. 2. The Poincaré map is again one dimensional. In Fig. 3 $\ln\Gamma$ versus $\ln l$ is plotted for selected values of q. A steplike structure can be observed. These steps have been observed by other authors when using the recurrence time measure[32] (see below). We think the origin of the steps is common to the fact that the crowding indexes always show a change of scaling (see Fig. 4), and are related to the finite number N of points on the attractor. In fact, the steps become more marked for larger values of q especially for negative ones, which clearly indicates a poorer statistic for the most rarified or concen-

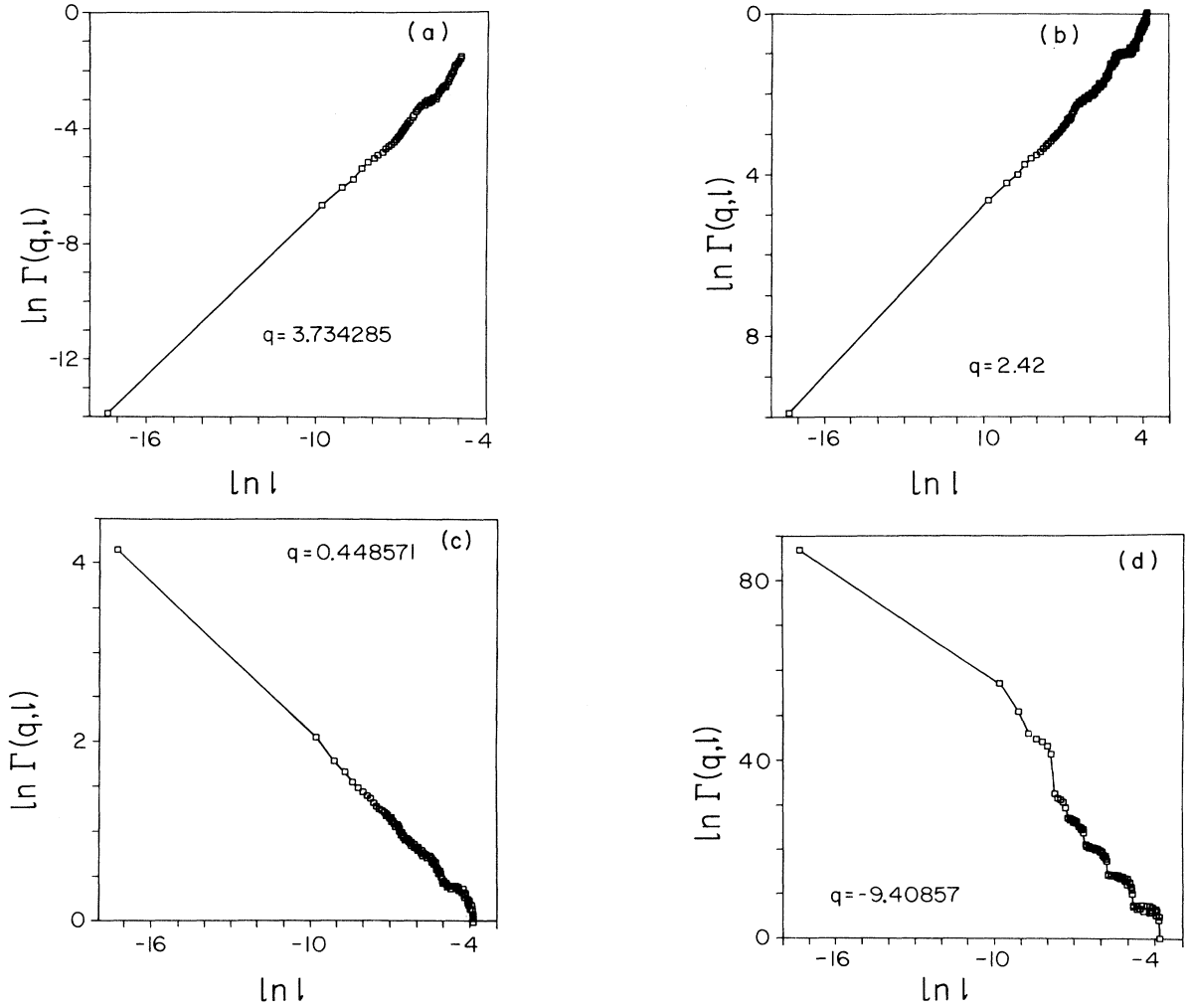

FIG. 3. (a)–(d) The partition function [Eq. (26)] is shown for selected values of q ($j_1=0.474\,890$). The steplike structure, which is more pronounced for negative q [(d)], is due to finite-size effects and in principle disappears in the thermodynamic limit $N\to\infty$. N is the number of points on the attractor.

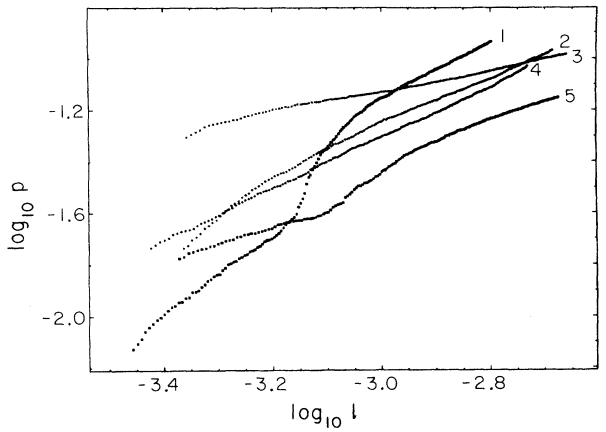

FIG. 4. The scaling curves around some selected points on the attractor of Fig. 12. Curve 1 has a top slope of 1.070 and a bottom slope of 1.47. Curve 2 has a top slope of 0.83 and a bottom slope of 1.80. Curve 3 has a top slope of 0.46 and a bottom slope of 0.32. Curve 4 has a top slope of 0.97 and the bottom slope shows no change of scaling. Curve 5 has a top slope of 0.81 and a bottom slope of 0.57.

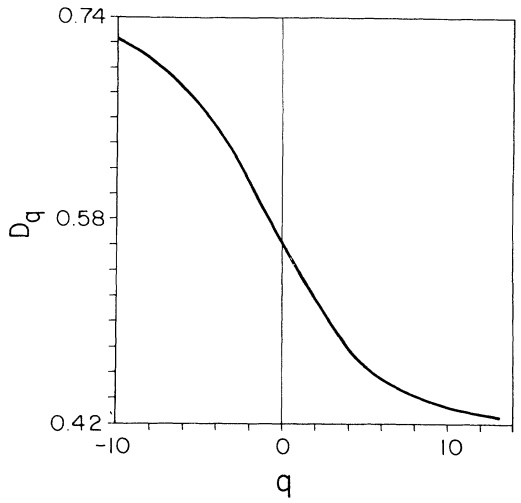

FIG. 6. The function $D_{(q)}$ is shown for the attractor at onset.

trated moments of the measure as q grows. The best fit to the plots gives us $\tau(q)$ from which we obtain the generalized dimensions D_q and the $f(\alpha(q))$ versus $\alpha(q)$ through a Legendre transformation

$$f(\alpha)=q\alpha-\tau(q),\quad \alpha=\frac{d}{dq}\tau(q),\quad q=\frac{d}{dq}f(q)\ . \tag{29}$$

However, if the function $\tau(q)$ is not differentiable one has to use the more general form

$$\tau(\alpha)=\inf[q\alpha-f(q)],\quad f(\alpha)=\inf[q\alpha-\tau(q)]\ . \tag{30}$$

The Legendre transform $f(\alpha)$ is the analog in thermodynamics to the entropy, α is the analog to the energy, and $\tau(q)$ is analogous to the free energy. Their singularities define phase transition points. However, our labeling of the boxes on the attractor in general does not correspond to the microstates. For that reason, and because we use averaged quantities, $\tau(q)$ and $f(\alpha)$ can at most give indications of a phase transition if present.

Figures 5, 6, and 7 show the functions $\tau(q)$, D_q, and the spectrum of scales $f(\alpha)$ obtained for the value $j_1=0.474\,890$. We find for the scales we have empirically used to obtain D_q and $f(\alpha)$ (Ref. 33) the universal values obtained for the Feigenbaum attractor.[8,34] This means that even for supercritical values, where the measure of the attractor has pieces (islands or bands) where it is continuous, the universal features of the Feigenbaum attractor can be seen on a scale that is larger than the island

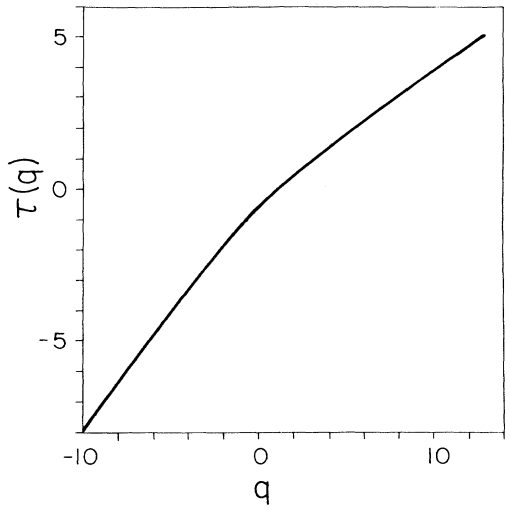

FIG. 5. The function $\tau(q)$ is shown for the attractor at onset.

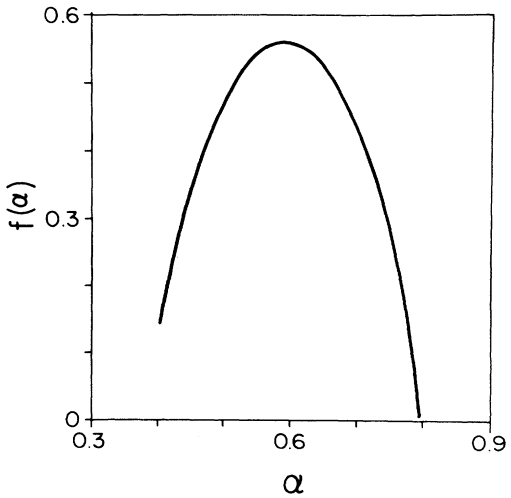

FIG. 7. The function $f(\alpha)$ is shown for the attractor at onset. The functions $\sigma(q)$, $D_{(q)}$, and $f(\alpha)$ corresponds to the universal Feigenbaum attractor.

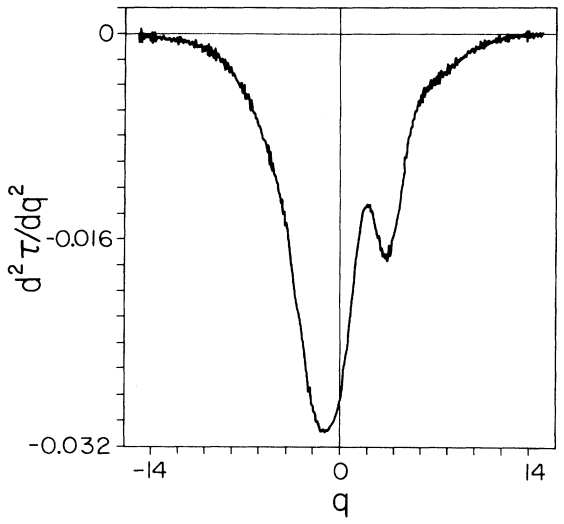

FIG. 8. The second derivative of $\tau(q)$ for $j_1=0.474\,890$.

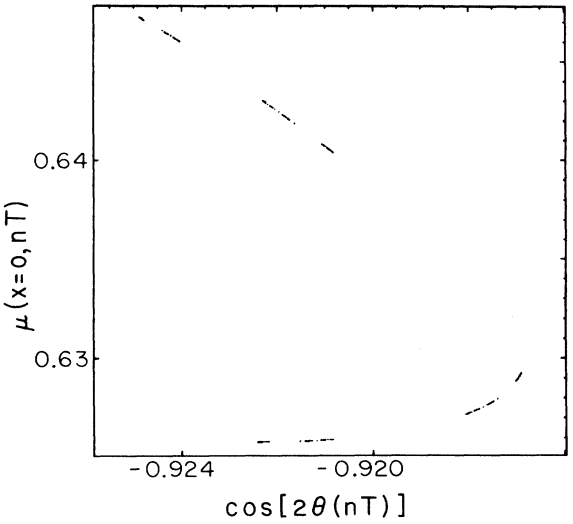

FIG. 10. The Poincaré map for $j_1=0.474\,892$. It is topologically equivalent to the Feigenbaum attractor.

width, i.e., the attractors behave on a coarse-grained scale like a physical object which can show multifractal scaling only on a finite range of length scales. Neither subcritical parameter deviations[35] nor finite-size effects at slightly supercritical values have qualitative relevance. In fact, it has been shown[36,37] that in the case of the logistic map for finite arbitrary small supercritical deviations there are bifurcations where band merging occurs (this happens at parameter values where the critical point is mapped into the unstable fixed point by a some iterate of the logistic map). In between, higher-order unstable orbits cause intermittency and band merging can be thought of as a collision of attractors with unstable periodic orbits (UPO). Some authors[27,38] have shown that, similar to the case of the logistic map $x_{n+1}=1-ax_n^2$, $a=2$, there also exists a phase transition at band merging. In that case the invariant measure has two singularities and it is possible to show analytically[39] that D_q has a discontinuity at $q=2$; this is equivalent to a phase transition (see below). For typical chaos[27] the invariant measure has a countable number of singularities. It is because of the different scaling of the probability measure at the valleys and the corners of islands that there is a discontinuity in D_q. The discontinuity is at $q=2$ because of the square-root singularity of the invariant probability measure.

Because of the averaging and coarse graining we cannot see the effect of these singularities on the $f(\alpha)$ curve, although it is evident in the histogram (Fig. 2). Notwith-

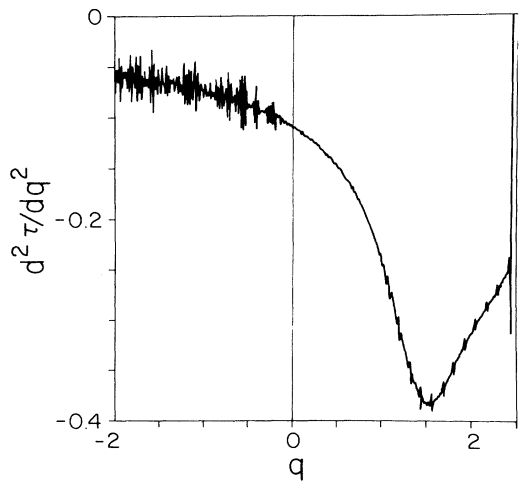

FIG. 9. The second derivative of $\tau(q)$ for $j_1=0.474\,55$.

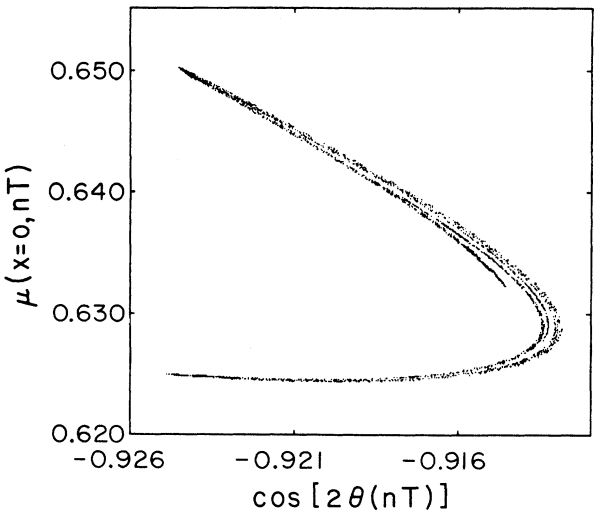

FIG. 11. The Poincaré map for $j_1=0.474\,84$. Note the appearance of foliations as the islands fuse.

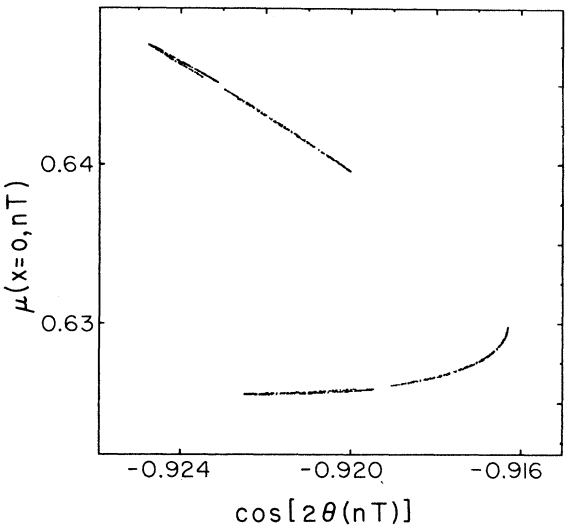

FIG. 12. The Henón-like Poincaré map for $j_1=0.474\,55$.

standing, the second derivative of $\tau(q)$ shows two peaks (Fig. 8). As our methods can give only an indication of a discontinuity, the bigger peak can be interpreted as an incipient of a singularity.[33] The smaller peak seems to be related to the saddle orbit of period 2^n for some unknown $n \gg 1$, which exists before the tangency occurs and collides with the attractor. The local expansion rates appear to be such that they produce hot spots[40] of high enough density so that their contributions to (19) peak over the other contributions. However, this peak does not diverge as $N \to \infty$, contrary to what is stated in Refs. 37, 41, and 42. It belongs to the hyperbolic phase. This means that the expansion rates of saddle points cannot produce phase transitions. Only marginal stable orbits can do this.[43]

It is interesting to note that the magnitude of the peaks is rather small (compare with Fig. 9 of this paper and Fig. 2 in Ref. 44). The reason for this could be the comparatively large distance from the bifurcation or band splitting. On the other hand, the singularity has the expected scale for the attractor at $j_1=0.474\,55$ [Fig. 9, (see below)].

Numerical simulations with the logistic map and Hénon map show similar features. Also found in ordinary differential equations (ODE) are features such as the resistive shunted junction (RSJ) model and the Duffing equations.[37,41]

The Poincaré map for values slightly below j_{ons} ($j_1 \cong 0.474\,88$) is already a multivalued function. The increasing folding probably begins for values arbitrarily small below j_{ons}. In Figs. 10–12 the Poincaré maps for $j_1=0.478\,92$, $0.474\,84$, and 0.48455 are shown. We conjecture that the homoclinic tangencies between the stable (W_s) and unstable (W_u) manifold of UPO lying in the fundamental neighborhood of the attractor are responsible for this gradual foliation. What happens is qualitatively the same as the mapping of the critical point by an n-times interate of the logistic map to the unstable fixed point, i.e., there is a homoclinic tangency. As the unstable manifold of an unstable periodic point pokes through the stable manifold there exists an intermittency.[36]

VI. PHASE TRANSITIONS AND SYMMETRY-INCREASING BIFURCATIONS BEYOND ONSET ($j_1 < j_{\text{ons}}$)

In principle, the way to prove the existence of a phase transition for the attractors defined by the Poincaré map[17] would be to find an encoding or symbolic dynamics for the calculation of the partition function (microstates). Such an encoding would give an optimal covering at the attractor to be contrasted with the ones defined above. The singularities in the associated thermodynamic functions define the phase transitions.[23] We will study such an encoding through the organization of the unstable periodic orbits in another work.[45]

We have used the method described in Sec. V, which smooths possible singularities. However, the calculated $f(\alpha)$ curves show a quasilinear region, which in fact can be interpreted as an indication of a phase transition.[43,46] However, this sort of diagnostic is not strong enough.

The fundamental point and main argument are the postulated tangency of W_u and W_s of a certain UPO. Such tangencies cause the formation of regions where the natural measure of the attractors have *abnormally* high densities (analogous to the singularities of the measure of the logistic map discussed above). Therefore, the pointwise dimension $\alpha(x)$ (Ref. 27) has a low value at the tangency point (nonhyperbolic point). This value is isolated from other values and in general the dimension $f(\alpha)$ of such points is finite. The tangency points define a nonhyperbolic part of the partition function [Eq. (19)]. We use this fact to diagnose the tangencies. Such an idea was already used to study $\alpha(x)$ at the turnbacks of the Hénon map[47] and to establish a theory of first-order phase transition.[43] We examine as an example the attractor for $j_1=0.474\,55$ shown in Fig. 12. The $f(\alpha)$ curves show a linear part for positive q. The $d^2\tau(q)/dq^2$ curve shows an incipient singularity at some q (Fig. 9). We choose random points on a attractor and study the crowding indexes [Eq. (24)]. Some representative curves are shown in Fig. 4. The important fact is the existence of a scaling for points near the turnback of the attractor, where the values of the $\alpha(x)$ are considerably smaller than the average $\langle\alpha(x)\rangle$ on the attractor and the most important are *less than* 1 [$\langle\alpha(x)\rangle$ gives $D_{q=1}$, the information dimension, and equals 1.45]. The last remark constitutes our main argument for the phase transition. This is because points on the attractor of the unstable manifold of saddle periodic orbits also produce values which differ from $D_{q=1}$, but they are never less than 1 (Ref. 48) and only pertain to the hyperbolic part of the partition function. These points, although called hot or cold spots, belong to the hyperbolic phase. For hyperbolic systems, the measure along the unstable direction is 1 and $D_q^u=1$ for q, i.e., $\alpha^u(x)=1$. The stable direction contracts to produce fractal measures, which is also the mechanism that produces $\alpha(x)$ less than 1. The topic deserves explanation: in calculating the pointwise dimensions we choose circles of radius l. The scaling for some points of the probability measure [Eq. (24)] with $\alpha(x)<1$

cannot be isotropic. The only way to achieve in two dimensions a scaling less than 1 is to make both partial dimensions[27] less than 1. This means that the folding and contraction are strong in both directions, such that they produce two Cantor sets for both partial dimensions. Here the overlapping of stable and unstable manifolds is involved, which makes possible the contraction along the unstable direction and also Cantor structure along the unstable direction. Note the change of scaling for some curves in Fig. 4. This feature is also found in hyperbolic systems. It just reflects the dominance in the scaling of different regions, e.g., by points of tangency or points on the unstable manifold of some saddle orbital of the LPM.[48]

We also find a symmetry-restoring or -increasing bifurcation at a value j_{SIB} near 0.473 65; i.e., at some value of j_1 the two conjugated chaotic attractors merge into one, which has, on average, an inversion symmetry. The signature is the presence of only odd multiples of ω in the FFT of $\mu(0,t)$. Compare Figs. 13 and 14. The strobscopic plots of $\mu(0,t)$, Fig. 15, for $j_1=0.470$, contrast with the one for $j_1=0.474\,55$, Fig. 16, with and without the symmetry, as can be seen. Phase plots of $(\mu(0,t),\sin[2\vartheta(0,t)])$ also show the presence on average of an inversion symmetry. However, the symmetry cannot be seen in the Poincaré map P (Fig. 17). Clearly, to see this symmetry we have to use the $P\odot P^*$ map, where $\odot$ denotes the composition.

Qualitatively we can model the findings with a two-dimensional map,

$$x_{n+1}=ax_n-x_n^3-by_n,\quad y_{n+1}=x_n\ . \tag{31}$$

This map has an inversion symmetry, like (16). The cubic nonlinearity resembles the nonlinear term on the right-hand side of Eq. (1). Qualitatively this map describes the Poincaré map (17) for a range of currents. The map shows a symmetry-breaking bifurcation (SBF) and a period-doubling cascade to chaos. For a parameter value a_{SIB}, while keeping the value of b fixed, the two conjugated attractors connected by the inversion symmetry merge into one with a natural measure with inversion symmetry.[15,16,36] This happens when the W_u and W_s of the fixed point (0,0) touch in a tangency. For sufficiently small values of b, this tangency occurs before the tangency of the W_u and W_s of the period-two fixed points by which the basin of attraction of the attractor at infinity penetrates that of the chaotic attractor and, therefore, it is not observable. For this model map the effect of the tangencies in changing the foliation of the attractors can be studied at least numerically, and probably the structure of the W_u and W_s corresponding to higher-order periodic orbits can also be studied. We detect at a_{SIB} [where the tangency of $W_u(0)$ and $W_s(0)$ occurs] $\alpha(x)$ values less than 1, as should be expected. The possible role of heteroclinic tangencies, if any, in this model remains unclear.

The Poincaré map given in (17) appears to define an invertible two-dimensional map, at least for a range of current values j_1 down to 0.4730. It appears to be

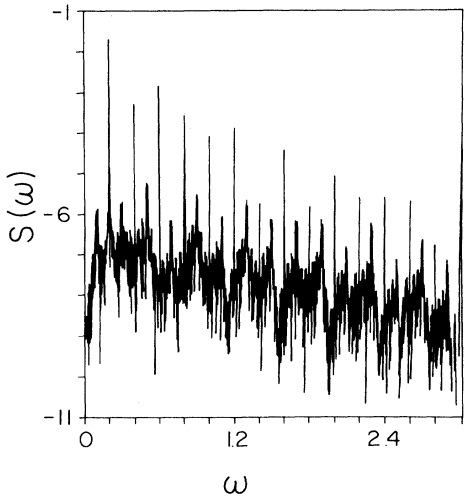

FIG. 13. The power spectrum of the attractor of Fig. 12. Note that all the harmonics are present.

Hénon-like[49] and nonhyperbolicity seems to be a pervasive feature as tangencies between stable and unstable manifolds occur all the way down from j_{ons} to j_{SIB}. However, it appears that high-dimensional behavior is starting to develop as the two-dimensional Poincaré map shows for $j_1=0.4715$ and $j_1=0.470$ (Figs. 17 and 18). In fact, this attractor has characteristic veils which indicate that it does not come from an invertible two-dimensional map. Attractor twisting can also be observed. Besides this, the coherence of the solution is softening and (17) projected to the first two components does not define a two-dimensional map anymore. This in-

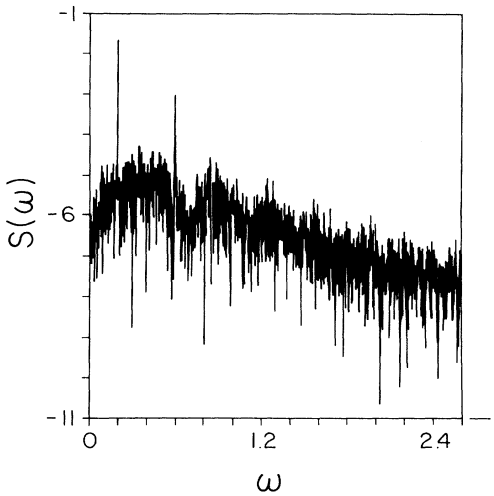

FIG. 14. The power spectrum of the attractor of Figs. 15 and 18. Only odd components of the fundamental frequency ($\omega=0.2$) are present, revealing the restoring of the symmetry of Eq. (15).

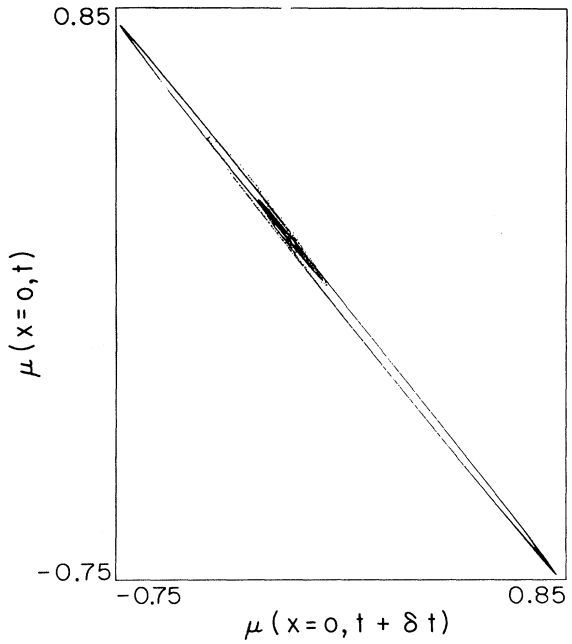

FIG. 15. The phase plot for $j_1=0.470$. Note the symmetry of Eq. (15).

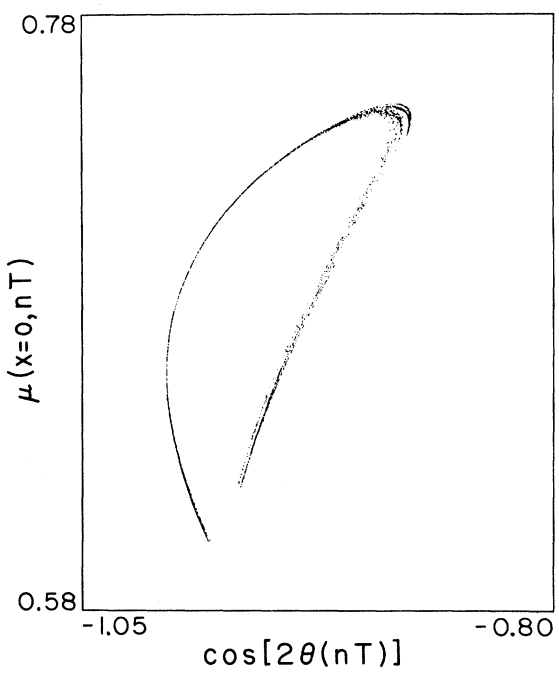

FIG. 17. The Poincaré map for $j_1=0.4715$. Although not clearly seen, the attractor has closed.

dicates a transition to what could be defined as soft turbulence[19] or to a behavior that can be related to at least three-dimensional maps.[50] Here our main conjecture for supercritical behavior (homoclinic tangencies) is not a necessary conduction for phase transitions.

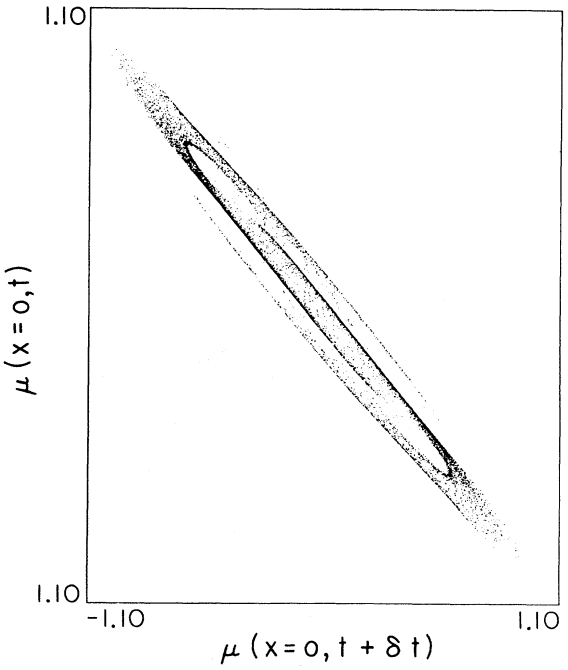

FIG. 16. The phase plot for a nonsymmetric attractor ($j_1=0.474\,555$).

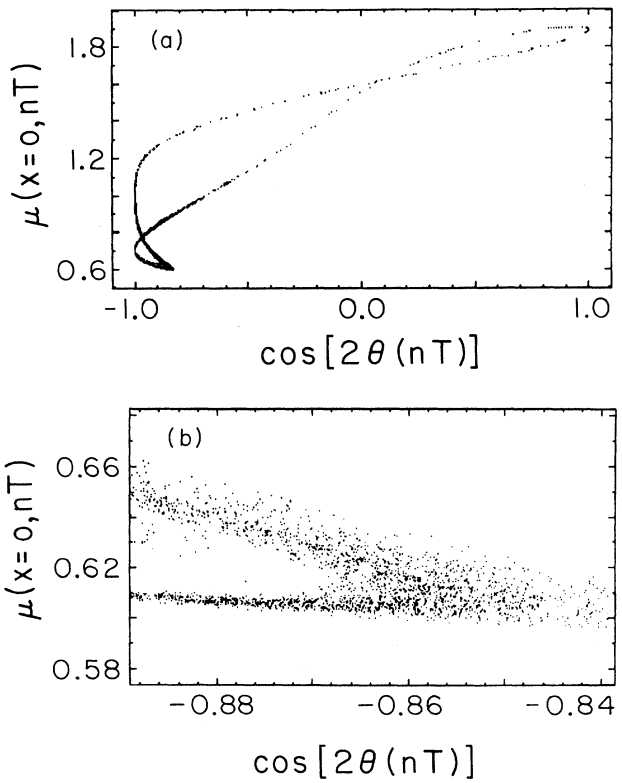

FIG. 18. (a) and (b) The Poincaré map for $j_1=0.470$. (b) shows the more dense part of the attractor with more detail. It does not have a Cantor structure and appears to completely fill the two-dimensional surface indicating higher dimensionality.

VII. CONCLUSIONS AND PERSPECTIVES

In this paper we have presented a detailed analysis of the transition to chaos (onset) and chaos beyond the transition in the low dissipative branch of ac-driven phase-slip-center solutions of the generalized time-dependent Ginzburg-Landau equations [Eqs. (1), (2), (3), and (13), and Fig. 1]. We studied the Poincaré map [Eq. (17)]. We found that this map behaves for a range of driving currents [Eq. (13), $0.4730 < j_1 < 0.490$] as a nonhyperbolic Hénon-like map.

We first calculated the multifractal spectrum of scaling exponents [Eqs. (24) and (25)] at the onset of chaos ($j_1 \cong 0.474\,892$). We find the universal spectrum of the Feigenbaum attractor. Second, for typical chaos (beyond onset), the behavior is qualitatively similar to the model map defined in Eq. (31). However, the folding structure of the LPM is much more dense than the model map.

The evaluation of the pointwise dimensions $\alpha(x)$ [Eq. (24)] results in a values less than 1. Also the thermodynamic function $d^2\tau(q)/dq^2$ shows an incipient singularity and the $f(\alpha)$ spectrum shows a quasilinear part. This is an accordance with a phaselike transition of first order.[43] The analysis of the model map also shows similar features. Therefore, we conclude that homoclinic tangencies are presented and are the primary reason for the phase transitions and attractor widening (foliation).

At $j_1 \cong 0.473\,65$ (j_{SIB}) a symmetry-increasing bifurcation occurs. This bifurcation reestablishes the symmetry (15), lost at the beginning of the period-doubling cascade, but in the average sense. This bifurcation is related to a homoclinic tangency.

For values less than j_{SIB}, the Poincaré map ceases to define a two-dimensional map (Figs. 17 and 18). This fact creates a very *promising perspective.* As has been recently pointed out,[50] higher-dimensional invariant manifolds and tangencies between any two one-dimensional stable manifolds can happen (in two dimensions this is not possible). This rules out nonhyperbolicity as the only source of phase transitions. As a result, nonisotropic effects[27] and even more structured measures could exist. This transition from local two-dimensional to three-dimensional behavior could bring new interesting aspects as important as the transition from a two- to three-dimensional system governing flows.[17]

Another point of interest concerns the biased case [Eq. (3), $j_0 \neq 0$]. Preliminary results[3] also confirm a universal transition from quasiperiodicity to chaos. We are also working on the universalities of the quasiperiodic case and thermodynamics at onset. Results on the characterization of chaos through the unstable periodic orbits and on the universalities related to intermittency at the symmetry-increasing bifurcation (natural measure and scaling lows, local expansion rates, etc.) are in progress. We are also working on the bifurcation behavior below the SIB. Details will be given elsewhere.

Finally we would like to remark that the described scenario can be used to explain the results at low dissipation for the generalized sine-Gordon equations.[19] This brings us to conjecture *generic behavior* in NPDE for chaos beyond onset after a cascade of period-doubling bifurcations. We believe our work could stimulate further experiments in this field.

ACKNOWLEDGMENTS

This work was partially supported by the Scientific Center IBM, Caracas. We express our gratitude to the Director of the Center, Dr. Juan Rivero, for his very helpful remarks and a careful reading of this work. We thank Dr. Miguel Octavio for his encouragement, for helpful discussions, and for a careful reading of this work. We also thank Ms. Lelis Ochoa and Lic. Pedro Silva for technical assistance.

[1]For a review, see V. P. Galaiko and N. B. Kopnin, in *Nonequilibrium Superconductivity,* edited by D. N. Langenberg and A. I. Larkin (North-Holland, Amsterdam, 1986).

[2]L. Kramer and R. J. Watts-Tobin, Phys. Rev. Lett. **40**, 1041 (1978); R. J. Watts-Tobin, Y. Krähenbühl, and L. Kramer, J. Low Temp. Phys. **42**, 459 (1981).

[3]R. Rangel, Ph.D. thesis, Universität Bayreuth, Freistaat Bayern, brd, Federal Republic of Germany, 1988.

[4]L. Kramer and R. Rangel, J. Low Temp. Phys. **57**, 389 (1984).

[5]M. Feigenbaum, J. Stat. Phys. **19**, 25 (1978); **21**, 669 (1979).

[6]P. Collet and P. Eckmann, *Iterated Maps of the Unit Interval* (Birkhauser, Zürich, 1980).

[7]M. Feigenbaum, L. P. Kadanoff, and S. J. Shenker, Physica D **5**, 37 (1982); H. G. Schuster, *Deterministic Chaos* (VCH Gesselschaft, Weinheim, Federal Repulic of Germany, 1988).

[8]Thomas C. Halsey, Mogens, H. Jensen, Leo Kadanoff, Itamar Procaccia, and Boris Shraiman, Phys. Rev. A **33**, 1141 (1986); D. A. Rand, Ergod. Theory Dynam. Syst. **9**, 527 (1989).

[9]G. H. Gunaratne, Paul S. Linsay, and Michael J. Vinson, Phys. Rev. Lett. **63**, 1 (1989).

[10]G. H. Gunaratne, M. H. Jensen, and I. Procaccia, Nonlinearity **1**, 157 (1988).

[11]H. Weissbrod, R. P. Huebener, and W. Clauss, J. Low Temp. Phys. **69**, 77 (1987). This work originally had mistaken concepts, which to apparent disagreement with the theory of Ref. 4. However, they corrected the results. See the Erratum: *ibid.* **73**, 171 (1988); see also Y. Yang and R. Tidecks, J. Low Temp. Phys. **70**, 131 (1988); U. Schulz and R. Tidecks, Solid State Commun. **66**, 59 (1988); B. Damaschke and R. Tidecks, J. Low Temp. Phys. **79**, 117 (1990).

[12]R. Tidecks and G. von Minnigerode, Phys. Status Solidi A **52**, 421 (1979); R. Tidecks, Ph.D. dissertation, University of Göttingen (1980).

[13]L. E. Guerrero and M. Octavio, Phys. Rev. A **37**, 3641 (1988); M. Octavio and L. E. Guerrero, *ibid.* A **42**, 4630 (1990).

[14]R. Rangel and L. Kramer, J. Low Temp. Phys. **74**, 163 (1989).

[15]Y. Yamaguchi, Phys. Lett. A **135**, 259 (1989), **A133**, 201 (1988); Y. Yamaguchi and N. Mishima, Phys. Lett. **109A**, 196 (1985).

[16]P. Chossat and M. Golubitsky, Physica D **32**, 423 (1988).

[17]J. Guckenheimer and P. Holmes, *Nonlinear Oscillations, Dynamical Systems and Bifurcations of Vector Fields* (Springer-Verlag, New York, 1983).

[18]G. Paladin and A. Vulpiani, Phys. Rep. **156**, 147 (1987).

[19]L. E. Guerrero and M. Octavio, Phys. Rev. A **40**, 3371 (1989).
[20]R. Rangel and L. Kramer, J. Low Temp. Phys. **68**, 85 (1987).
[21]A. J. Ritger, H. Meissner, R. Rangel, and L. Kramer, J. Low Temp. Phys. **73**, 221 (1988).
[22]J. W. Swift and K. Weisendfeld, Phys. Rev. Lett. **52**, 705 (1984); A. MacDonald and M. Plischke, Phys. Rev. B **27**, 201 (1983).
[23]G. L. Sewell, *Quantum Theory of Collective Phenomena* (Clarendon, Oxford, 1986).
[24]J. P. Eckmann and D. Ruelle, Rev. Mod. Phys. **57**, 617 (1985).
[25]The physical measure is defined as the zero noise limit of a mesaure ν obtained from the deterministic time evolution under the effect of an additional stochastic perturbation (Ref. 24). Actually the situation may be even more complex since here we are consistently neglecting noise effects by thermal fluctuations always present in experiments. For dc-driven phase-slip centers thermal fluctiation effects have been discussed. [L. Kramer and R. Rangel, J. Low Temp. Phys. **75**, 65 (1989)]. However, for conventional superconductors with low T_c one expects no major effects.
[26]H. G. E. Hentschel and I. Procaccia, Physica D **8**, 435 (1983).
[27]P. Grassberger, R. Badii, and A. Politi, J. Stat. Phys. **51**, 135 (1988).
[28]Jens Feder, *Fractals* (Plenum, New York, 1989).
[29]M. H. Jensen, L. P. Kadanoff, and A. Libchaber, Phys. Rev. Lett. **55**, 2798 (1985).
[30]R. E. Amritkar and N. Gupte, Phys. Rev. Lett. **60**, 245 (1988).
[31]K. Pawelzirk and H. G. Schuster, Phys. Rev. A **35**, 481 (1987).
[32]E. G. Gwinn and R. M. Westervelt, Phys. Rev. Lett. **59**, 157 (1987).
[33]P. Cvitanovic, *Phase Transitions on Strange Sets in Nonlinear Evolution and Chaotic Phenomena,* edited by G. Gallavotti and P. F. Zweigfel (Plenum, New York, 1989); R. Badii, Nuovo Cimento **10**, 819 (1988); Dwight Barkley and Andrew Cumming, Phys. Rev. Lett. **64**, 327 (1990).
[34]David Bensimon, Mogens, H. Jensen, and Leo P. Kadanoff, Phys. Rev. A **33**, 3622 (1986).
[35]M. G. Cosenza, W. D. McCormick, and J. B. Swift, Phys. Rev. A **39**, 2734 (1989).
[36]C. Grebogi, E. Ott, F. Romeiras, and J. A. Yorke, Phys. Rev. A **36**, 5369 (1987).
[37]H. Hata, T. Horita, and H. Mori, Prog. Theor. Phys. **82**, 897 (1989).
[38]David Katzen and Itamar Procaccia, Phys. Rev. Lett. **58**, 1169 (1987).
[39]E. Ott, W. B. Withers, and J. A. Yorke, J. Stat. Phys. **36**, 687 (1984).
[40]C. Grebogi, E. Ott, and J. A. Yorke, Phys. Rev. A **37**, 1711 (1988).
[41]S. Mayazaki, N. Mori, T. Yoshida, H. Mori, and T. Horita, Prog. Theor. Phys. **82**, 863 (1989).
[42]K. Tomita, H. Hata, T. Horita, H. Mori, T. Morita, H. Okamoto, and H. Tominaga, Prog. Theor. Phys. **81**, 1124 (1989).
[43]E. Ott, C. Grebogi, and J. A. Yorke, Phys. Lett. A **135**, 343 (1989).
[44]H. Hata, T. Morita, H. Mori, T. Morita, and K. Tomita, Prog. Theor. Phys. **80**, 809 (1988).
[45]The study of the unstable periodic orbits lying in the fundamental neighborhood will allow us to detect the relevant homoclinic tangencies.
[46]R. Stoop, J. Peinke, J. Parisi, B. Roehricht, and R. P. Heubener, Physica D **35**, 425 (1989).
[47]M. H. Jensen, Phys. Rev. Lett. **60**, 1680 (1988).
[48]Celso Grebogi, Edward Ott, and James A. Yorke, Phys. Rev. A **37**, 1711 (1988).
[49]P. Cvitanovic, G. H. Guranatne, and I. Procaccia, Phys. Rev. A **38**, 1503 (1988).
[50]P. Paoli, A. Politi, and R. Badii, Physica D **36**, 263 (1989).